JOM, Vol. 69, No. 4, 2017
DOI: 10.1007/s11837-017-2274-1

Study the Synthesis, Characterization and Immersion of Dense and Porous Bovine Hydroxyapatite Structures in Hank's Balanced Salt Solution

N. ESLAMI,[1] R. MAHMOODIAN,[1,2,5,6] M. HAMDI,[1,2,7] NADIA MAHMOUDI KHATIR,[3] M.K. HERLIANSYAH,[4] and ALI REZA RAFIEERAD[1,2]

1.—Department of Mechanical Engineering, Centre of Advanced Manufacturing and Materials Processing (AMMP), University of Malaya, Kuala Lumpur, Malaysia. 2.—Department of Mechanical Engineering, Faculty of Engineering, University of Malaya, 50603 Kuala Lumpur, Malaysia. 3.—Department of Biotechnology, Faculty of Biological Science, Alzahra University, Tehran, Iran. 4.—Department of Mechanical Engineering, Gadjah Mada University, Yogyakarta, Indonesia. 5.—e-mail: mahmoodian@um.edu.my. 6.—e-mail: mahmoodian.reza@gmail.com. 7.—e-mail: hamdi@um.edu.my

The bone-bonding potential of biomaterials is evaluated in vitro through examining the surface apatite formation in Hank's media to enhance biocompatibility, which is also applicable to facilitate in vivo osseointegration of implantable devices. Hence, bovine hydroxyapatite (BHA) bioceramic structures have been used in various biomedical applications such as orthopedic implants. In this article, the microstructure, in vitro bioactivity, and nanomechanical properties of the synthesized dense and porous BHA are investigated via scanning electron microscopy, x-ray diffraction, energy-dispersive x-ray spectroscopy, Fourier transform infrared spectroscopy, and nanoindentation analysis. From the obtained results, porous BHA mostly possesses adequate requirements for substitution as implants in the human body.

INTRODUCTION

Hydroxyapatite (HA), with the chemical formula $Ca_{10}(PO_4)_6(OH)_2$, is deemed a prominent bioceramic with various biomedical approaches.[1,2] Hence, because of its excellent biocompatibility, osteoconductivity, bioaffinity, and slow replacement response by the host after implantation, HA is widely considered in implant industries.[3] Concerned with the attractive characteristics of HA, several methods have been applied to chemical synthesize such wet-precipitation, continuous precipitation, hydrothermal, and sol-gel also extracting from natural human, animal, and plant resources.[4–6] In the case of obtained bovine HA (BHA) from animal bone structure, the derived powder possesses desired properties of real bone that provide the capability of direct bone formation. Moreover, the resulted biocompatible materials perform a rapid bone graft without allergenic and inflammation risk.[7] Based on the reported research, HA is capable of bonding directly to tissues and of promoting osseointegration feasibility of porous and dental implants for orthopedic and dental applications. Nevertheless, a main challenge of synthesized HA is its poor mechanical stability particularly in wet media.[8,9] Hence, its clinical targets are limited to low-load-bearing approaches such tooth replacement, filling periodontal pockets, the prosthesis regions adjacent to hard implants, spinal fusions, and nonunion of long bones.[10] More recently, scientists have focused on preparing hydroxyapatite with a porous morphology. Hence, a porous HA structure results in strong bonding with the host bone. In addition, the pores of such an implant help achieve a mechanical interlock that leads to more powerful material fixation.[11,12] For ideal osteointegration, the dimensions and porosity are reportedly considered the most important factors. The minimum pore size requirement for macro-pores to enable bone ingrowth with blood supply ranges from 100 μm to 150 μm.[13] Moreover, dense HA structures have been used in dentistry, percutaneous access assist devices (PADs), continuous ambulatory peritoneal

(Published online February 14, 2017)

dialysis (CAPD), and permanent space fillers to repair bone defects. Nonetheless, dense HA is mechanically brittle and can only be used in low-mechanical-stress applications. HA materials boast a strong structure with acceptable mechanical properties and can bond rapidly with the host. Yet, several limitations exist, such as low absorbability during application.[14] To assure stability of the bone-like implant and rapid osseointegration, biomaterials are required to possess the biocompatibility potential for reasonable durability. Thus, BHA with mimic natural bone properties is applied to rehabilitate bone defects and create stable bonding amid an implant and a natural bone as biodegradable features. It is reported that the integrated bone-like cement prevents the failure loosing by filling the clearance space. The current mechanism suggests that the reaction may involve higher absorption of calcium (Ca) and phosphors (P), and the improved fracture resistant can be corresponded to for stability and durability of implanted devices.[15]

Herein, two morphologies of BHA bioceramic materials (dense and porous) were successfully developed from bovine bone. The dissolution behavior of both BHA samples was investigated by immersing the samples into calcium-free Hank's balanced salt solution for certain periods of time. Moreover, the nanomechanical properties of BHA were determined in terms of nanoindentation and nanoscratch analysis. The results of this investigation are expected to provide information on the characteristics of natural-biological origin bioceramics, especially the dissolution behavior of BHA bone graft. This shall become the first step toward producing low-cost BHA bone graft products for biomedical applications.

EXPERIMENTAL PROCEDURE

BHA Powder Preparation

Cortical bovine bones were collected from local slaughterhouses. To avoid soot formation in the material during heating and to remove organic substances and collagen using boiling followed with sun drying was compulsory. The dried cortical bone samples were cut and heated in air atmosphere at 900°C for 2 h with a temperature rate of 5°C min^{-1}. The cooled bovine bone pieces were crashed using mortar pestle and sieved to obtain BHA powder with a particle size less than 400 μm.

Dense and Porous BHA Preparation

Dense BHA samples were produced by compacting BHA powder at 156 MPa into pellet bodies using cylindrical dies (D = 20 mm). The compacted green bodies were pressureless sintered in an atmospheric furnace with heating and cooling rates of 5°C min^{-1} at 1200°C for 2 h. In addition, the porous samples were fabricated by using a planetary ball milling of the bovine bone powder with 30 wt.% coarse sucrose powder as a porogen. Afterward, the obtained mixture was uniaxial pressed under the same conditions as the dense samples. Likewise, the compressed green bodies were pressureless heat treated under the mentioned sintering conditions.

Surface Characterization

The morphology and microchemistry features as well as the Ca/P ratio transformation of the specimens' surface before and after immersion in Hank's solution were investigated with scanning electron microscopy (SEM, INCA Energy 200, Oxford Institute), Changes on the surface morphologies and microstructure of the samples before and after immersion were characterized by environmental scanning electron microscopy (SEM, INCA Energy 200, Oxford Institute), energy-dispersive x-ray spectroscopy (EDX, INCA Energy 200, Oxford Institute), and microanalysis Suit V4.05 software, respectively. Furthermore, the detected phases in the dense and porous structures were analyzed by x-ray diffractometer (XRD, Siemens D5000, Germany) with CuKα radiation power of 50 kV, 300 mA, and scan rate of 0.02° s^{-1}. The nanomechanical properties of the specimen were conducted using the Berkovich indenter of the Triboscope system (Hysitron Inc., USA). The ISO 14577 standard was implemented for nano-indentation and scratch analysis.[16]

Immersion Test

The immersion test was carried out according to a related study by Pourbaix on the corrosion behavior of materials used as implants. Herein, focus was placed on the vital role of Ca/P dissolution and precipitation in bioceramic bone graft as well as on biocompatibility assessment in body media.[17] Therefore, based on the physiological issues related to the potential of hydrogen (pH) considerations, Hank's solution is used to examine the in vitro bioactivity through dissolution of HA as an oxide layer biomaterial. As a result, immersion analysis of both dense and porous BHA bioceramic structures was conducted in a calcium-free composition of Hank's balanced salt solution.[13] Dissolution analysis was also performed by immersing the BHA samples with both structures into separate, sealed polyethylene bottles containing 20 mL of Hank's body simulated solution with the composition presented in Table I and pH of 7.4 (Sigma Aldrich Company, St. Louis, MO).

It is worth noting that the volume of each bottle was sufficient to accommodate the immersed samples, which were kept in an incubator at near-body temperature of around 36.5°C for 3 days, 8 days, 16 days, 28 days, and 36 days. After the specimens were soaked for the predetermined intervals, they were removed from the solution, gently washed with deionized water, and phosphate-buffered saline (PBS) to remove residual solution and subsequently dried at room temperature.

Table I. Composition of Hank's balanced salt solution

Constituent	KCl	KH_2PO_4	NaCl	$NaHCO_3$	$Na_2HPO_42H_2O$
Gram/liter	0.40	0.06	8.00	0.35	0.06

RESULTS AND DISCUSSION

Microstructure Analysis

The observed SEM morphologies of synthesized dense and porous BHA before and after 16 days and 36 days' immersion in Hank's balanced salt media are illustrated in Fig. 1. The offered micrographs of dense surfaces (Fig. 1a,b) as well as the porous condition (part c, d) before soaking into the body-simulated solution display rough surfaces with almost no macropores, cracks, and precipitating particles except a few with diameters of less than 5 μm. In addition, with respect to the reported results by Salgado et al.,[18] related to the various chemical and physical properties of bioceramic materials such surface roughness and pores topography, the effects of cellular adhesion and proliferation are important aspects worth investigating in the stability of implant materials.[19] Accordingly, after 16 days' immersion of dense and porous BHA, the surfaces started to exhibit apatite precipitation (part e, h). Such a mechanism reaction of material precipitation that results in creating a thick layer of apatite with a Ca/P ratio of 0.7–2.3 and a superiority of porous structure was introduced without any pretreatment of the samples in alkaline solution. This effect plays a key role on bone ingrowth and on the implant fixation bone-like apatite layer, which was also in agreement with Kokubo and Takadama's research.[20] Gradually, by increasing the immersion time to 32 days, the concentration of precipitating materials increased on the surface, as demonstrated in parts g and l for dense and porous samples, respectively. Moreover, the thick agglomerates formed on the BHA surface, which behave as a bone-like apatite layer discussed by EDX analysis that confirmed the Ca/P ratio of the apatite film is 2.3, which is higher than that in pure HA. This issue is linked to the formation of carbonate hydroxyapatite on the surface. In the case of porous BHA, the surface is completely covered with a thick apatite layer without any pretreatment in body-simulated solutions that was assisted by the higher apatite formation affected by higher absorption of Ca and P to induce the heterogeneous nucleation phenomena, which plays a key role in bone ingrowth and implant fixation.[21,22]

The initial cracks first appeared on the surface after some primary immersion time. It is obvious that the number of cracks and precipitation increased. This phenomenon, which is addressed by the dissolution reaction, followed the research conducted by Fazan and Marquis et al.[23] The crack distribution with different immersion times for both dense and porous BHA structures highly affects the mechanical properties.[24] Higher magnifications of SEM morphology may contribute to distinguishing the surface roughness of BHA before and after immersion processes. Again, the pores contained macro and micro structures, yet no cracks were observed on the surface. In regard to the enhanced precipitation process in the case of porous BHA structures, it can be deducted from the morphology formed that Ca/P precipitated not only in the top area of the porous BHA surface but it also deposited inside the macropore structure.

Structural Characterization

Figure 2a and b illustrates the XRD patterns and detected phases in the dense and porous BHA specimens for both initial and final states of immersion in Hank's balanced salt solution. The detected peaks were identified using standard code JCPDS 9-432, the crystalline stoichiometric HA, and JCPDS No. 9-348 for triclacium phosphate (α-TCP). The main phase transformation of α-TCP was mainly occurred after sintering at a range of 1000°C to below 1100°C. Thus, in the diffraction pattern of these dense BHA samples, a crystalline HA peak and two weak α-TCP peaks can be mostly indexed. The XRD patterns of as-received bovine bone present the nanocrystalline apatite in bone matrix. With increasing the sintering temperature to 600°C, the apatite peaks gradually appeared in the XRD pattern. The phase analysis of a bone-like structure at a higher annealing temperature matched to 700°C, 800°C, 900°C, and 1000°C were assessed with similar reported results at 600°C and matched with the dominant substantial pattern with raised and reduced peaks in height and width, respectively.[9] Thus, indicating an increase in crystallinity and crystallite size at a higher temperature followed in this research. All the XRD signatures for BHA samples were in agreement with the stoichiometric HA characterized pattern (XRDJCPDS data file No. 9-432). In addition, thermal treatment at above 1100–1200°C lead to partial phase decomposition of HA to pattern minor calcium phosphate phases (β-TCP). When 1200°C was reached, the current intensity of characterized HA peaks appears for the β-TCP phase, which are located at angular 2θ positions of 27.78, 31.18, 44.58, and 47.78 subsequently. The phase characterization confirmed that the stability in the bone matrix was not disrupted when annealed in air up to 1000°C. The sintering

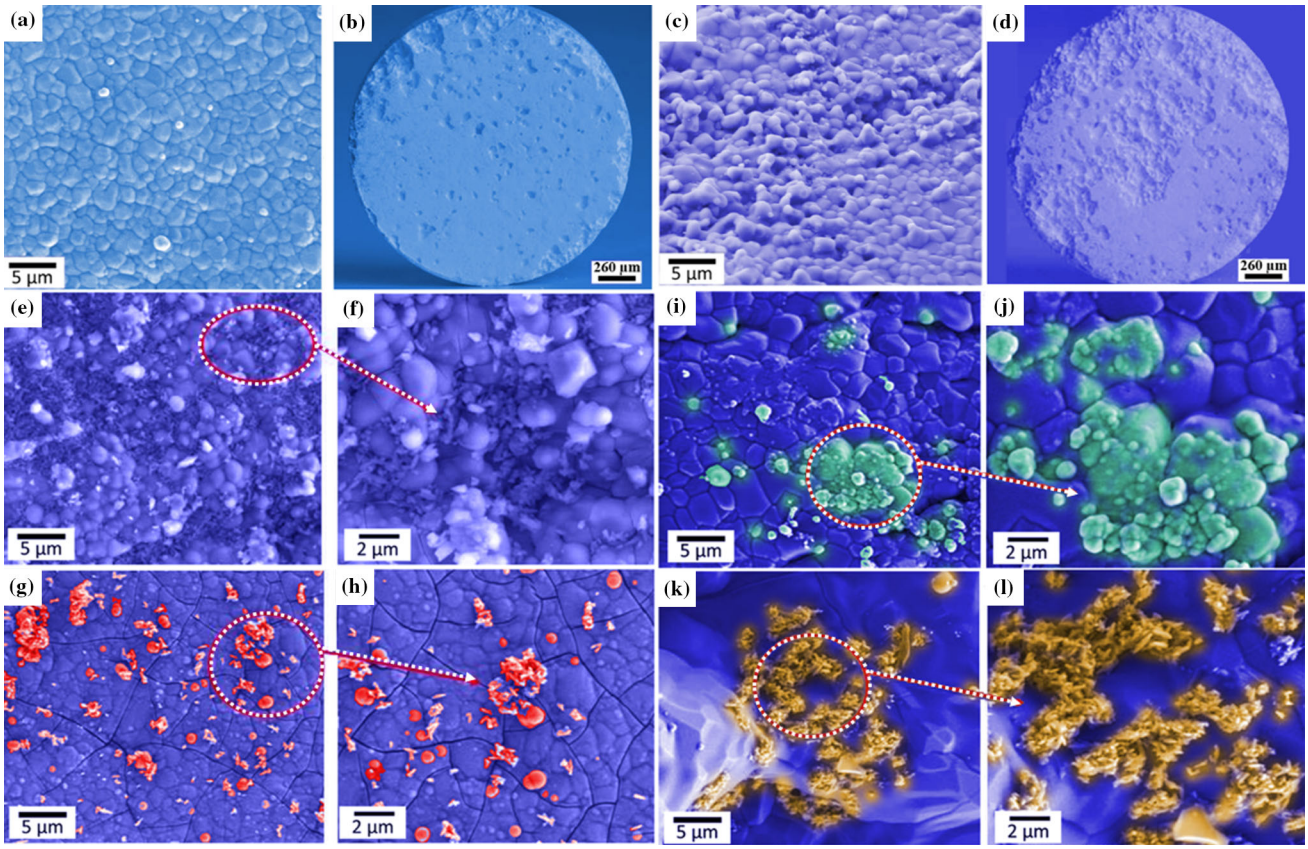

Fig. 1. SEM micrograph images of BHA structures (a, b) dense and (c, d) porous before immersion, and for dense BHA 16 days' immersion in Hank's balanced salt solution (e, f), 32 days (g, h), and case of porous BHA (i, j) 16 days and (k, l) 36 days.

transition of BHA samples at 1200°C provided the stability of developed artificial bone materials with higher intensity in the case of porous samples. Accordingly, after the immersion step, the BHA structures were reinforced with a formed appetite structure that represents the considered chemical absorption process within saturated Hank media. Most HA peaks were supposed to be intact even after 36 days of immersion, indicating that the HA phase did not degrade. Nevertheless, the presence of α-TCP (500) and (511) weak peaks in the dense BHA samples immersed for 28 days indicates that these samples slightly degraded due to released Ca and P ions into body-simulated solution. In direct relation with the porous samples marked part (b), all peaks from the porous BHA sample before immersion were identified more strongly using JCPDS No. 9-432, indicating they belonged to the crystalline stoichiometric HA with no other impurities detected until 16 days of immersion. After immersion for 28 days, the analysis process was repeated and it was found that the number of HA peaks decreased but α-TCP peaks appeared. The presented graphs prove that after 28 days of immersion, the dissolution process became dominant compared with the previous precipitation process.

Elemental Analysis

Figure 3 demonstrates the elemental composition and transformation ratios of Ca/P and EDX analysis attached with SEM observation for dense and porous BHA structure, before and after immersion in Hank's solution. Based on obtained EDX results related to elemental analysis and Ca, P, and O concentrations, it can be concluded that the thick apatite layer was created on the surface of both BHA structures with different elemental concentrations. This assessment may contribute to the capability of quick osseointegration for orthopedic implant materials. In terms of decreasing Ca and P content ratios within the porous structures for the different immersion times, the dissolution of related samples appears higher than that of the dense samples. This is likely the reason for the higher decrement of Ca and P content in the porous state rather than in the dense structures.

Nanomechanical Properties

The nanomechanical properties of the specimen were determined in terms of nanoindentation and Nanoscratch tests.[25,26] To examine the strength properties of synthesized BHA, the ISO 14577 standard was implemented for nanoindentation.

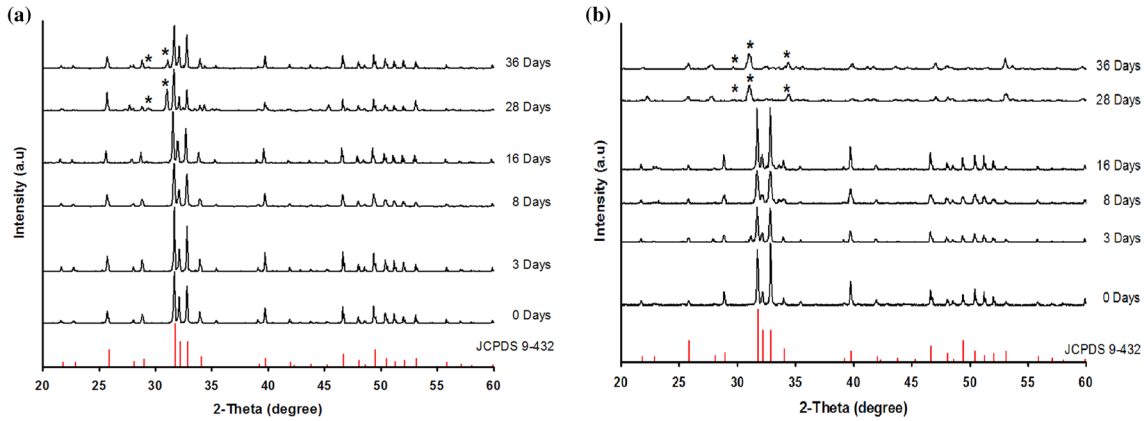

Fig. 2. XRD graph and detected phases of dense BHA (a) and porous samples (b) before and after various immersion time in Hank's solution, TCP (tricalcium phosphate) [*].

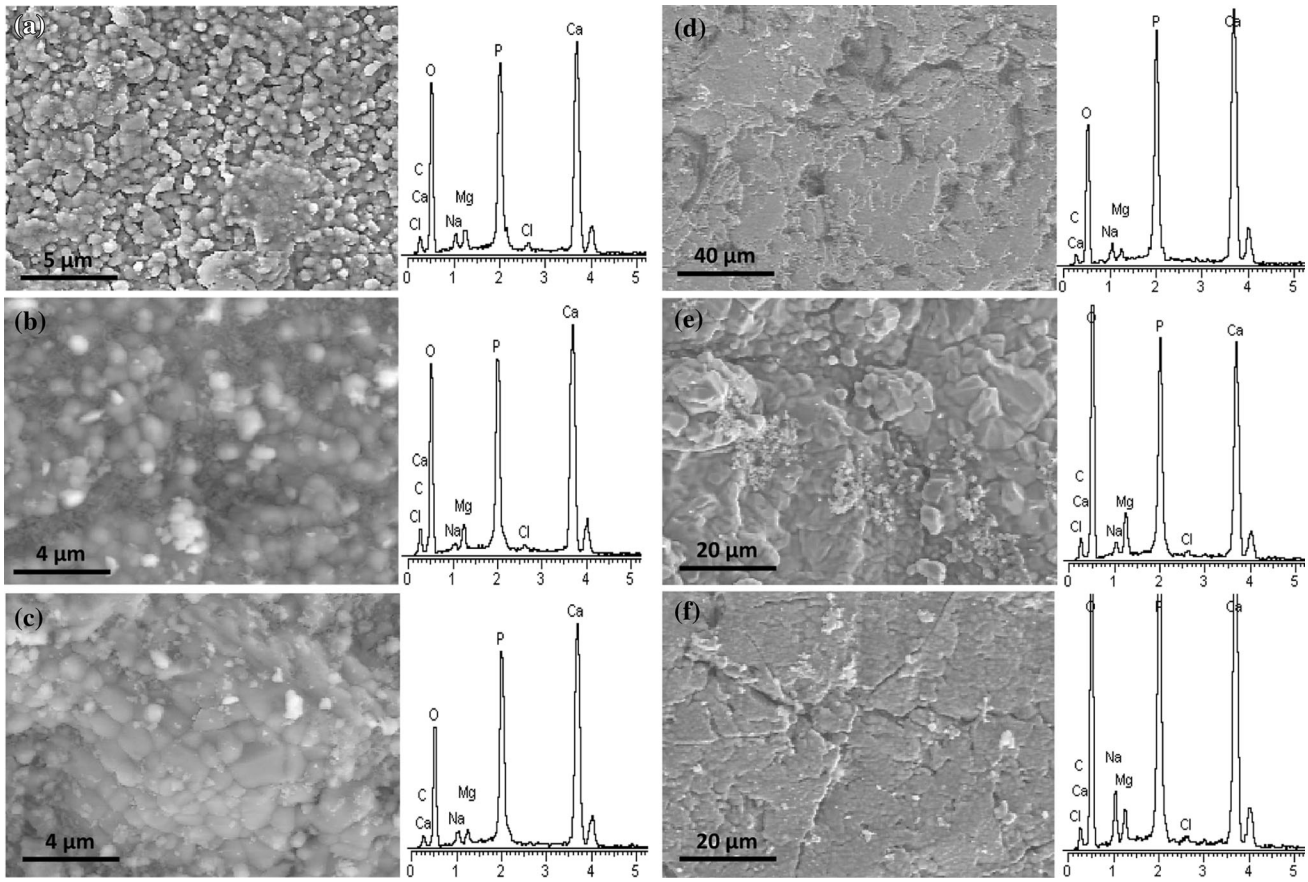

Fig. 3. EDX graphs of dense BHA structure (a) before, (b) after 16 days, and (c) after 36 days and for porous sample (d) before, (e) after 16 days, and (f) after 36 days of in vitro bioactivity analysis.

The applied parameters were involved by maintaining a constant indentation depth. The speed for each loading and unloading step was also kept constant. The nanoscratch parameter on the specimens was set at a penetration load of 4000 μN and a constant scratch speed of 0.13 μN s^{-1} with 4 μm of scratch length and indenter penetration depth of 150 nm. The nanoscratch hardness was measured at 7.0 ± 0.3 GPa and normal hardness of 6.0 ± 1.1 GPa. Moreover, Fig. 4a and b represents the effect of immersion time on the calcium and phosphorous concentrations for both dense and porous BHA structures, whereas Fig. 3 demonstrates that calcium and phosphorous content in the related samples decreased as a result of longer immersion time. The content of the mentioned

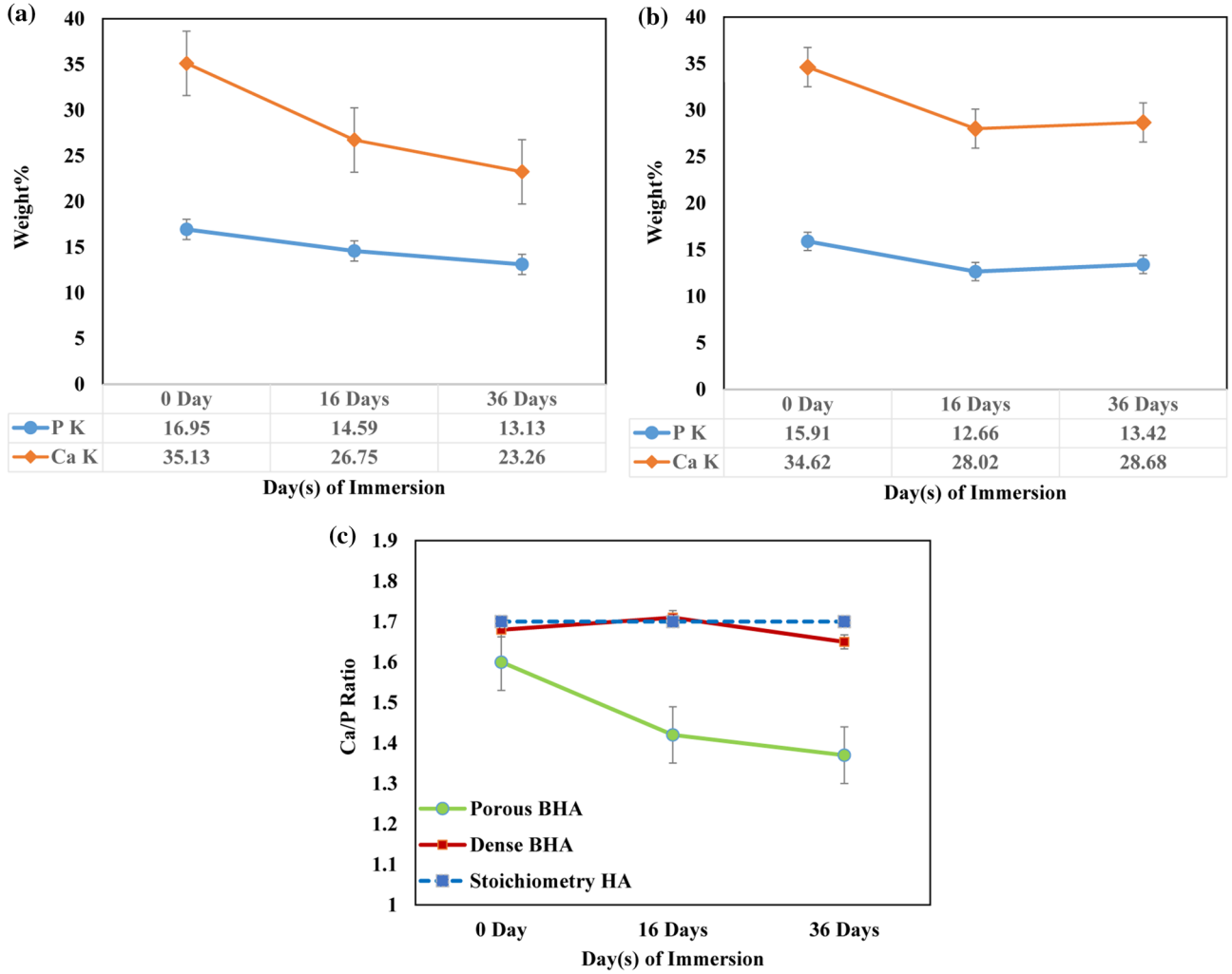

Fig. 4. Effect of immersion time on the calcium and phosphorous concentrations in (a) dense and (b) porous structures when (c) compared with stoichiometric HA.

elements rapidly decreased from the initial state (before immersion) until 16 days of immersion. Nonetheless, with this amount of time, the Ca and P content decreased slightly as represented by the low graph slope in Fig. 4c for Ca and P content after immersion for 16–36 days.

The changes in Ca and P content in the dense BHA structure samples highly affected the Ca/P ratio. Remarkably, the dense BHA samples had a Ca/P ratio of 1.68 before immersion in Hank's solution. It is worth noting that the related Ca/P ratio is closer to the Ca/P ratio of standard stoichiometric HA equations. These results are also supported by the XRD graphs and detected phases of dense BHA structure samples in the primary immersion condition (JCPDS 9-432) for stoichiometric HA. When the dense BHA structure samples were immersed for 36 days, the Ca/P ratio shifted to 1.65 (part c). Additionally, these results match the results reported by Kokubo and Takadama, which indicate the apatite layer precipitates on the surface.[20] The same comparison amid mechanical properties of real bone and synthesized BHA from natural resources could be also applicable for investigation of the suitability of the sintered BHA biomaterials in practical and implant applications. In addition, the examined reasonable aspects of developed bone-like structures are not valuable unless the desired nanomechanical characteristics are being sacrificed within a minimum number of experiments and costs. Therefore, these analysis methods may be considered to be appropriate alternatives for tribological investigation of BHA structures.

Chemical Compounds and FTIR Analysis

All functional groups in the BHA structure samples before and after immersion in Hank's solution were determined via Fourier transform infrared spectroscopy (FTIR). The FTIR graphs of dense and porous BHA samples are illustrated in Fig. 5a and

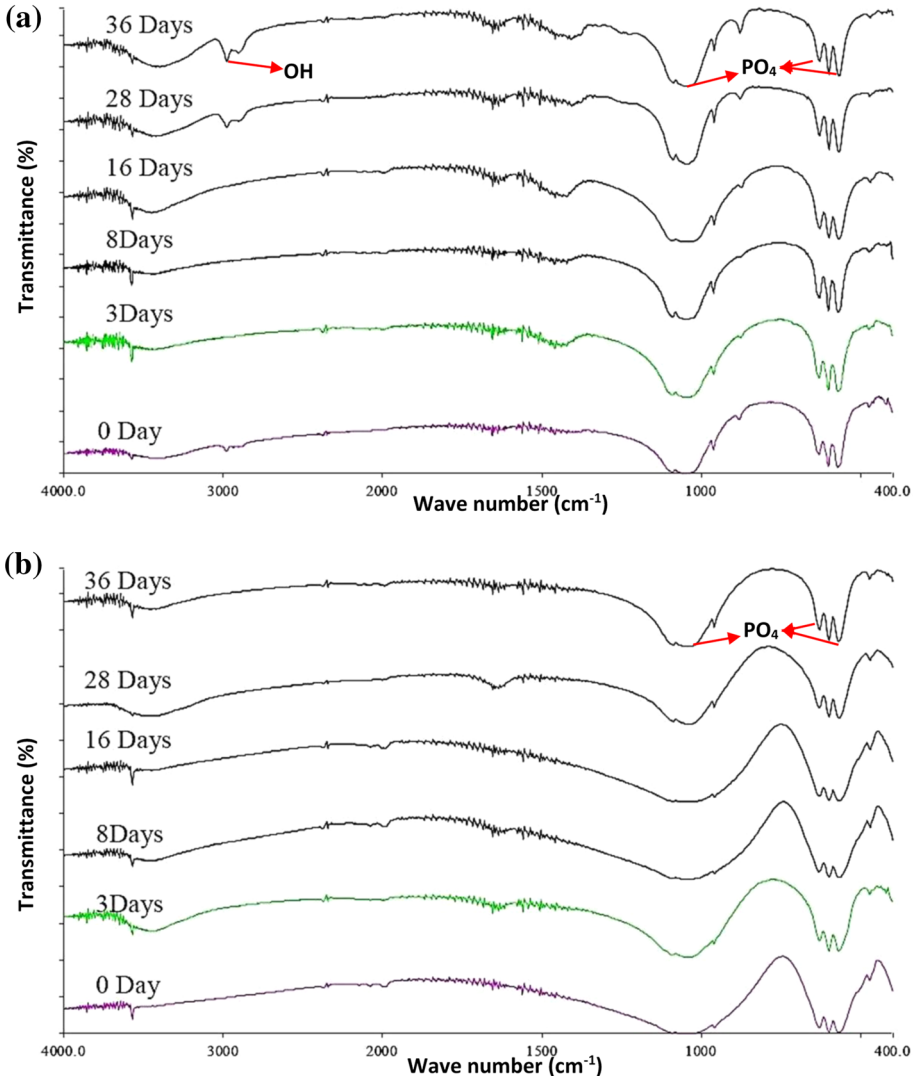

Fig. 5. FTIR graphs of dense (a) and porous (b) BHA before and after immersion in Hank's solution.

b, respectively, for various immersion times (0 day, 3 days, 8 days, 16 days, 28 days, and 36 days). Evidently, the results obtained from FTIR for dense samples before immersion are in complete agreement with the HA reference spectrum. In the case of dense BHA, the related spectra bands of 570 cm^{-1} and 603 cm^{-1} that completely matched the vibration of PO_4 observed during all spectrums gradually increased with a longer immersion time. Nevertheless, the group band of OH exhibited no changes during the immersion process. Moreover, the absorption band's intensity (961 cm^{-1}) slightly increased through the immersion process, which is indicative of a clear PO_4 content increment. Hence, it is deducted that the band at 879.26 cm^{-1} is directly linked to carbon (C) content. The wide peak (1034–1150 cm^{-1}) features observed for α–TCP stayed constant until 16 days of immersion; after which (28 days and 36 days of immersion), they increased but at a low rate. The considered peaks that appeared after 28 days and 36 days of immersion at 2940 cm^{-1} and 2985 cm^{-1} matched with the OH group, which signifies the absorption of samples into the solution.

It is obvious from the obtained results that by immersing BHA in Hank's solution, $CaHPO_4$ precipitated in the solution and gradually came up to the sample's surface. Hence, the PO_4 present was absorbed in the dense BHA samples after 28 days and 36 days. These results are also in line with the EDX and XRD results for dense samples. The phosphorus content was evident at a higher rate after 16 days of immersion. TCP peaks were observed in the related graphs for 28 days and 36 days. The changes in the spectrums after immersion were insignificant. The related band at 476 cm^{-1} completely matched the vibration of PO_4 as observed in all graphs. The considered code in the FTIR graphs at 570 cm^{-1} and 603 cm^{-1} also completely matched the PO_4 amounts. In addition, there

was a weak band in all spectrums at 879 cm^{-1} like for the dense state, which is related to carbon content. The wide peak observed at the 1034–1150-cm^{-1} features of α–TCP did not change after 16 days of immersion, but after 28 days and 36 days, the considered value significantly increased. The widest FTIR band observed was detected at 3400–3570 cm^{-1}, which corresponds to the OH group. Furthermore, a wide band appeared three days after immersion in Hank's solution, meaning that absorption occurred after the immersion process. According to obtained results, the porous structure in porous BHA samples provided a wider contact surface compared with dense samples, which amplifies the higher dissolution rate of Ca^{2+} ions in the porous structure.

CONCLUSION

In this work, development of dense and porous BHA bone graft from animal resource was carried out. The microstructural morphologies, phase transformation, and bioactivity properties were characterized to confirm the stability of synthesized implant materials. The in vitro dissolution activity of dense and porous BHA structures was also examined by immersing in Hank's balanced salt solution for different periods of time comparably. The crystallinity of the samples in immersion also affected dissolution, and the amorphous phases showed a more soluble trend than did crystalline CaP apatite formation. The produced structures were crystalline apatite, causing a slower dissolution rate and precipitation in these materials compared with both amorphous and crystalline film materials sintered at 1200°C. The morphology results of BHA represent macropores with an approximate size of around 400 μm and micropores present in the BHA bone graft, which may cause nanomechanical properties to show around 6- to 7-GPa hardness. The dissolution rate of porous samples was higher than that of dense samples, which resulted in a lower Ca/P ratio in porous samples than in dense samples with the longer immersion time. In a nutshell, green development of a porous BHA structure with superior performance rather than a dense condition may contribute in orthopedic applications as desired biodegradable ceramic material. The higher mechanical properties of a porous BHA structure with functionalized carbon-based materials reinforcement will be considered as future work to enhance the BHA performance.

ACKNOWLEDGEMENTS

The authors would like to acknowledge the University of Malaya for providing the necessary facilities and resources for this research by Postgraduate Research Fund (Grant PG266-2015B) and the Ministry of Higher Education, Malaysia Fundamental Research Grant Scheme (FP059-2015A).

REFERENCES

1. S.M. Londoño-Restrepo, C.F. Ramirez-Gutierrez, A. del Real, E. Rubio-Rosas, and M.E. Rodriguez-García, *J. Mater. Sci.* 51, 9 (2016).
2. A. Dabbagh, R. Mahmoodian, B.J.J. Bin Abdullah, H. Abdullah, M. Hamdi, and N.H. Abu Kasim, *Int. J. Hyperthermia* 31, 8 (2015).
3. A.R. Rafieerad, M.R. Ashra, R. Mahmoodian, and A.R. Bushroa, *Mater. Sci. Eng. C* 57, 397 (2015).
4. C. Kothapalli, M. Wei, A. Vasiliev, and M. Shaw, *Acta Mater.* 52, 19 (2004).
5. M. Manassero, A. Decambron, N. Guillemin, H. Petite, R. Bizios, and V. Viateau, *Coral Scaffolds in Bone Tissue Engineering and Bone Regeneration, The Cnidaria, Past, Present and Future* (New York: Springer, 2016), pp. 691–714.
6. W.-F. Ho, H.-C. Hsu, S.-K. Hsu, C.-W. Hung, and S.-C. Wu, *Ceram. Int.* 39, 6 (2013).
7. E. Chee, Y.-D. Kim, K.I. Woo, J.H. Lee, J.H. Kim, and Y.-L. Suh, *Ophthal. Plast. Reconstr. Surg.* 29, 2 (2013).
8. B. Nasiri-Tabrizi, A. Fahami, and R. Ebrahimi-Kahrizsangi, *Ceram. Int.* 39, 5 (2013).
9. C. Ooi, M. Hamdi, and S. Ramesh, *Ceram. Int.* 33, 7 (2007).
10. M. Prakasam, J. Locs, K. Salma-Ancane, D. Loca, A. Largeteau, and L. Berzina-Cimdina, *J. Funct. Biomater.* 6, 4 (2015).
11. B. Flautre, M. Descamps, C. Delecourt, M. Blary, and P. Hardouin, *J. Mater. Sci. Mater. Med.* 12, 8 (2001).
12. Y. Li, T.T. Thula, S. Jee, S.L. Perkins, C. Aparicio, E.P. Douglas, and L.B. Gower, *Biomacromolecules* 13, 1 (2011).
13. T. Yoshii, M. Yuasa, S. Sotome, T. Yamada, K. Sakaki, T. Hirai, T. Taniyama, H. Inose, T. Kato, Y. Arai, S. Kawabata, S. Tomizawa, M. Enomoto, K. Shinomiya, and A. Okawa, *Spine* 38, 10 (2013).
14. M.R. Ayatollahi, M.Y. Yahya, H.A. Shirazi, and S.A. Hassan, *Ceram. Int.* 41, 10818 (2015).
15. J. Mahamid, A. Sharir, D. Gur, E. Zelzer, L. Addadi, and S. Weiner, *J. Struct. Biol.* 174, 3 (2011).
16. R. Mahmoodian, M.A. Hassan, S. Ghadirian, and M. Hamdi, *Combust. Sci. Technol.* 186, 6 (2014).
17. M. Hamdi and A. Ide-Ektessabi, *Mater. Sci. Eng. C-Bio S* 27, 4 (2007).
18. A.J. Salgado, O.P. Coutinho, and R.L. Reis, *Macromol. Biosci.* 4, 8 (2004).
19. J.-H. Lee, J.-H. Kim, and J.-H. Jeon, *Implant Dent.* 24, 3 (2015).
20. T. Kokubo and H. Takadama, *Biomaterials* 27, 15 (2006).
21. A. Rafieerad, A. Bushroa, B. Nasiri-Tabrizi, J. Vadivelu, S. Baradaran, M. Mesbah, and M.A. Zavareh, *Mater. Des.* 103, 10 (2016).
22. M. Sainz, P. Pena, S. Serena, and A. Caballero, *Acta Biomater.* 6, 7 (2010).
23. F. Fazan and P.M. Marquis, *J. Mater. Sci. Mater. Med* 11, 12 (2000).
24. S. Naderi, M.A. Hassan, and A.R. Bushroa, *Mater. Des.* 67, 360 (2015).
25. M.A. Hassan, A. Bushroa, and R. Mahmoodian, *Surf. Coat. Technol.* 277, 216 (2015).
26. M.A. Hassan, R. Mahmoodian, and M. Hamdi, *Sci. Rep.* 4, 3724 (2014).